consist *only* of a Q-branch, non-totally symmetric Raman bands with distinct Q-branches were observed (see STOICHEFF [3], p. 140 f.; HOLZER [4], HOLZER and MOSER [5]). However even if the Q-branch in the rotational structure of non-totally symmetric Raman bands would be generally missing (which actually is not at all the case) this hardly could be considered as a logically consistent argument for the non-totally symmetric vibrations to be forbidden in the Raman effect. The well-known fact that the totally symmetric lines in the Raman spectrum usually have the highest relative intensities has to be explained in another way (see [6], p. 108). If non-totally symmetric vibrations would appear in the Raman spectrum only because of intermolecular interactions, the intensity ratio of non-totally to totally symmetric lines ought to increase when changing from the gaseous to the liquid state. However the contrary was observed (see e. g. PERZL and MOSER [7], Table 1 and 2; HOLZER [8]).

[3] B. P. STOICHEFF, Advances in Spectroscopy (Edited by H. W. THOMPSON), Vol. 1, Interscience 1964, pp. 91—174.
[4] W. HOLZER, Diplomarbeit, Munich 1964.
[5] W. HOLZER and H. MOSER, J. Mol. Spectr. **13**, 430 [1964].
[6] J. BEHRINGER, Theorie der molekularen Lichtstreuung, Sektion Physik d. Universität München, Lehrstuhl Prof. BRANDMÜLLER, 1967.
[7] F. PERZL and H. MOSER, J. Mol. Spectr. **26**, 237 [1968].
[8] W. HOLZER, Dissertation (Thesis), Munich 1967.

Range of Validity of Static Potential Approximation in Low-Energy Electron Scattering Checked by Cross Section Measurements of Hg between 25 and 150 eV

W. EITEL, K. JOST *, and J. KESSLER

Physikalisches Institut, Universität Karlsruhe

(Z. Naturforsch. **23 a**, 2122—2123 [1968]; received 10 October 1968)

A renewed interest in low-energy electron scattering has become evident in the past few years. One of the problems under discussion is: In which energy range can those theories [1–3] be regarded reliable which make the simplifying assumption that scattering takes place in the static (relativistic Hartree) potential of the atom.

SCHONFELDER [4] had claimed that for mercury this approximation is no longer valid for energies below 500 eV. The present authors [5, 6] showed, however, that this limit is too high, since between 500 and 100 eV there is very good agreement between theoretical predictions and experimental results. The differential cross sections communicated in the present paper display the transition from the energy range where the theories still hold to the energy range where they break down.

The experimental procedure for obtaining these cross sections has been described earlier [6, 7] and can be summarized as follows: An electron beam crosses a mercury atomic beam by which some of the electrons are scattered. The density of the atomic beam is made low enough so that single scattering is ensured [7]. By rotating the electron gun, the scattering angle is varied continuously. The angular resolution for the present measurement is about $\pm 2°$. The scattered beam first passes through an energy filter lens which removes inelastically scattered electrons. Then the beam enters a Faraday cup and, after amplification, the intensity I versus scattering angle Θ is recorded by an XY-recorder.

From these measurements the relative cross sections $d\sigma/d\Omega$ were obtained by multiplying the scattered intensity I by $\sin\Theta$, since the effective path length of the

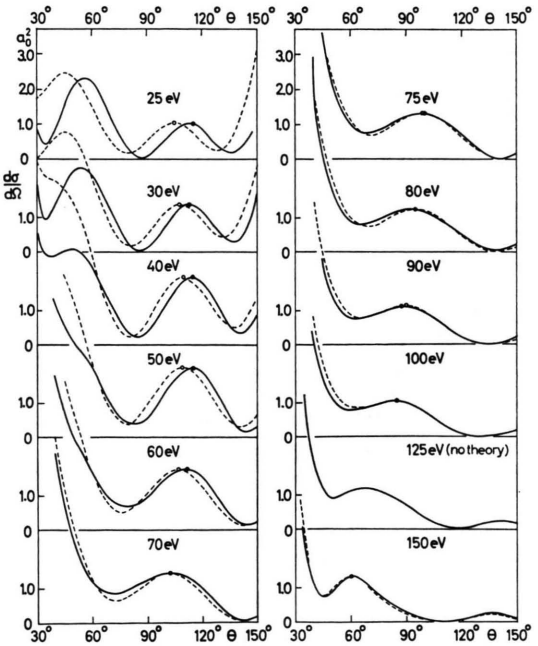

Fig. 1. Differential cross sections for elastic electron scattering by mercury between 150 and 25 eV. Solid line, experiment, dashed line, theory of Coulthard and Walker. At the points marked by a circle, the ordinate of each experimental curve has been normalized to the corresponding theoretical one (a_0 = Bohr radius in hydrogen).

* Present address: Stanford University, Stanford, California.
[1] G. HOLZWARTH and H. J. MEISTER, Nucl. Phys. **59**, 56 [1964].
[2] P. J. BUNYAN and J. L. SCHONFELDER, Proc. Phys. Soc. London **85**, 455 [1965].
[3] D. W. WALKER, Phys. Rev. Letters **20**, 827 [1968].
[4] J. L. SCHONFELDER, Proc. Phys. Soc. London **87**, 163 [1965].
[5] W. EITEL, K. JOST, and J. KESSLER, Phys. Rev. **159**, 47 [1967].
[6] K. JOST and J. KESSLER, Z. Physik **195**, 1 [1966].
[7] W. EITEL, K. JOST, and J. KESSLER, Z. Physik **209**, 348 [1968].

electrons in the scattering chamber is proportional to $(\sin\Theta)^{-1}$ in the angular range considered here. For comparison with theory, the ordinate of each experimental curve was normalized to the corresponding theoretical one in one point (maximum) which is marked by a small circle.

Fig. 1 gives the results. The theoretical data have been obtained by COULTHARD and WALKER (private communication) by the partial wave method using the relativistic Hartree potential for mercury. One can see that only at energies lower than about 70 eV, the discrepancies begin to become significant. There the angular shift between theoretical and experimental curves, which has been found earlier [8] also at higher energies, increases rapidly, and even the shapes of the two kinds of curves begin to differ from each other. At the lowest energies shown here the discrepancies must be regarded serious. At even lower energies there is little or no correlation between experimental and theoretical curves, as shown by SCHONFELDER [4] on the basis of the measurements by DEICHSEL et al. [9].

The results show that the theories which assume the scattering to take place in the static potential of the atom are no longer reliable at the lower energies considered here, although their range of validity extends to energies which are by an order of magnitude lower than earlier expected [4]. Exchange and correlation effects due to electron spin and charge polarization of the atomic electron cloud probably are the cause of these discrepancies. Recently YATES and STRAND [10] calculated differential cross sections for argon, krypton, and iodine considering also exchange between incident and atomic electron. Comparison of their results for argon with the differential cross sections measured by MEHR [11] down to 20 eV showed at energies below 40 eV a strong sensitivity of the cross sections to the exchange interaction.

The large discrepancies at low energies demonstrate that it would be important to have theoretical calculations which include the effects so far neglected (like exchange, charge polarization, correlation), particularly since experimental data are now available which can be used for comparison.

The authors are indebted to the Deutsche Forschungsgemeinschaft and the Bundesministerium für wissenschaftliche Forschung for support.

[8] A survey of the earlier measurements can be found in: J. KESSLER, Rev. Mod. Phys. **41**, No. 1 [1969].
[9] H. DEICHSEL, E. REICHERT, and H. STEIDL, Z. Physik **189**, 212 [1966].
[10] A. C. YATES and T. G. STRAND, Phys. Rev. **170**, 184 [1968].
[11] J. MEHR, Z. Physik **198**, 345 [1967].

Bestimmung höherer Potentialkoeffizienten des Hinderungspotentials von Molekülen mit zwei Methylgruppen

A. TRINKAUS, H. DREIZLER und H. D. RUDOLPH

Physikalisches Institut der Universität Freiburg i. Br.

(Z. Naturforsch. **23 a**, 2123—2124 [1968]; eingeg. am 31. Oktober 1968)

Die Beschreibung des Hinderungspotentials durch mehrere Potentialkoeffizienten wird bei dieser Molekülklasse erschwert durch:

a) die geringe Intensität der Übergänge in höher angeregten Torsionszuständen,

b) das Fehlen klarer Zuordnungskriterien infolge größerer Aufspaltung der Multipletts (Zusammengehörigkeit wegen Überlappung oft nicht mehr ersichtlich),

c) Schwierigkeiten in der Anwendung der „Bootstrap"-Methode zur Berechnung der Störsummen für die in der Basis zweier unabhängiger Teilkreisel $\psi_{v_1\sigma_1}\cdot\psi_{v_2\sigma_2}$ entarteten Niveaus, z. B. $v\,v'=01$ und 10, falls beide Teilkreisel äquivalent sind.

Im folgenden wird ein Rechenverfahren beschrieben, das die Bestimmung höherer Potentialkoeffizienten ermöglicht. Es verwendet im Effekt als Basis für den Torsionsanteil die Lösungsfunktionen eines Systems zweier *gekoppelter* Teilkreisel $\Phi_{(vv')_{\sigma_1\sigma_2}}$ [1] an Stelle der $\psi_{v_1\sigma_1}\cdot\psi_{v_2\sigma_2}$.

[1] $(v\,v')$ symbolisiert die aus der vorher entarteten Gesamtheit entstandenen Zustände.

Der Hamilton-Operator lautet:

$$H = A\,P_a^2 + B\,P_b^2 + C\,P_c^2 + F_1\,\mathcal{P}_1^2 + F_2\,\mathcal{P}_2^2 + F'(\mathcal{P}_1\mathcal{P}_2 + \mathcal{P}_2\mathcal{P}_1) \tag{1 a}$$

$$\left.\begin{aligned} &+F_1\,p_1^2 + \tfrac{1}{2}V_3(1-\cos 3\alpha_1)\\ &+F_2\,p_2^2 + \tfrac{1}{2}V_3(1-\cos 3\alpha_2)\\ &+F'(p_1\,p_2 + p_2\,p_1) + V_{12}\cos 3\alpha_1\cos 3\alpha_2\\ &+V_{12}'\sin 3\alpha_1\sin 3\alpha_2 + \ldots \text{ (höhere Terme)}\end{aligned}\right\} \tag{1 b}$$

$$-2F'(p_1\mathcal{P}_2 + p_2\mathcal{P}_1) - 2F_1\,p_1\mathcal{P}_1 - 2F_2\,p_2\mathcal{P}_2\,. \tag{1 c}$$

Es bedeuten:

$g=x,y,z.$	Die Indizes bezeichnen körperfeste Hauptträgheitsachsen des Moleküls.
I_g	Hauptträgheitsmomente des Moleküls.
I_{ai} $(i=1,2)$	Trägheitsmomente der Teilkreisel um ihre Symmetrieachse.
λ_{gi}	Richtungskosinus zwischen der Achse des i-ten Teilkreisels und der g-ten Hauptträgheitsachse.
P_g	g-Komponente des Gesamtdrehimpulses.
p_i	Komponente des Gesamtdrehimpulses des i-ten Teilkreisels, entlang seiner Drehachse.

$$\mathcal{P}_i = \sum_g \frac{\lambda_{gi}\,I_{ai}}{I_g}\,P_g\,.$$

v_i	Torsionsquantenzahl des i-ten Teilkreisels.
σ_i	Symmetrieindex der Torsionseigenfunktionen des i-ten Teilkreisels.
α_i	Torsionswinkel des i-ten Teilkreisels.